A new world map for wave power with a focus on variability

John V. Ringwood
Centre for Ocean Energy Research
Maynooth University, Ireland
E-mail: john.ringwood@eeng.nuim.ie

Gabriel Brandle
Ecole Centrale de Nantes
Nantes, France
E-mail: gabriel.brandle@hotmail.fr

***Abstract*—Traditionally, sea areas with a high mean wave power, ideally situated close to population centres, are seen as the most viable for harnessing economic wave energy. However, wave energy variability is a key driver of cost, since significant variation above the mean power will have implications for system rating and capacity and the capability to withstand high loads. Conversely, significant variation below the mean with result in ineffective power conversion, due to the robust nature of a wave energy converter with an ability to deal with high loads. Additional benefits of low power variability include smoother power production and increased value of generated electrical power. This paper demonstrates a prototype wave map which features wave power variability as a central figure of merit in the search for suitable wave energy sites. In particular, the coefficient of variability is introduced as a key metric. An on-line prototype map has been developed with a range of key information provided at a number of locations at which data was made available.**

***Index Terms*—Wave energy, wave map, variability, wave power, coefficient of variability**

I. Introduction

Given the escalating energy needs of the world and the concern over emissions from the burning of fossil fuels, a significant amount of focus has been brought to bear on the as-yet untapped wave energy resource. Of particular interest is the extent of the wave energy resource, which has been quantified in a number of publications, including [1], [2], [3]. In general, an assessment is made of the (annual) average wave power in TW, or the total wave energy over a particular period (e.g. a year) in TWh. Exceptionally, some shorter averaging period is used (such as quarterly) in order to get a measure of the seasonality of the wave resource [1]. Further studies have been carried out in the assessment and quantification of the global wave energy resource, including [21], which has a focus on raw mean wave power and average convertible power/energy using a Pelamis model and [22], which uses the phase-average spectral Wavewatch III data [28], [23], with again a focus on mean quantities (period and height), though monthly quantities are also considered. The impact of these studies is twofold, in that (a) they confirm that the wave resource is significant and worth harnessing as a serious energy contributor, and (b) that specific areas in the world have better wave resources than others.

With regard to (b) above, prospective wave power project developers may look for high (average) power wave energy sites close to population centers which maximise the commercial viability of wave power projects, either for electricity production or potable water production. By choosing a location close to a population centre and/or a major port and/or a strong grid connection, transmission (and installation and maintenance) costs may be minimised and energy receipts maximised. Typically, the following costs [4] for wave energy projects are articulated:

- Capital costs
  - Devices
  - Foundations/Moorings
  - Connections
  - Project costs
  - Decommissioning
- Operating costs
  - Maintenance
  - Operations
  - Insurance
  - Seabed rent
  - Transmission charges

while income related to annual energy production depends on site resources, device energy capture and availability. [5] and [6] also document costs and economic flows for wave energy projects.

Peak-to-average ratio (PAR) has been identified as a major cost driver in wave energy systems [7] and other renewable energy application areas [8]. PAR for wave energy is also regarded as large and difficult to predict [9] and it is notable that some studies on the economics of wave energy do not explicitly itemize PAR as a cost driver [4], [6]. Nonetheless, the ability to capture peak power clearly adversely impacts capital costs and, if the PAR is large, the corresponding average energy receipts will be relatively small, compared to the plant capacity. In addition, the ability to either match the natural dynamics of a wave energy converter (WEC) to the predominant (most frequently occurring) sea state is largely a function of the device mass, which may have to artificially large in order to cope with peak sea conditions. Intuitively, it would be hard to imagine that a device able to handle the sea conditions shown in Fig.1 (either in power production mode, or survival mode) could also operate efficiently in moderate to light wave conditions.

ISSN 2309-1983

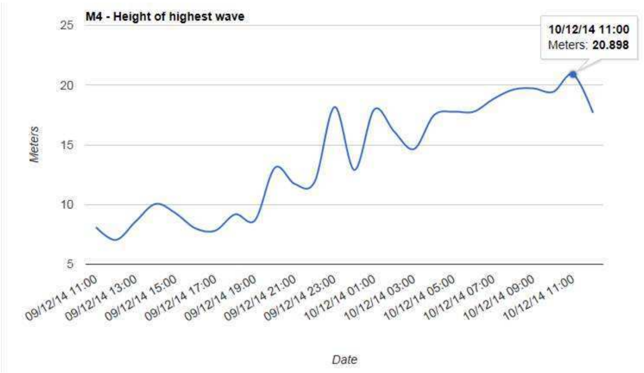

Fig. 1. Peak wave heights from the M4 databuoy off the West Coast of Ireland (Data courtesy of the Irish Marine Institute)

A reasonable example of how a system can be optimised at a particular operating point can be had by examination of a conventional thermal power plant. The device components are all designed to have maximum efficiency at rated power and the plant is normally operated at rated power, but never at a power level exceeding rated power. Therefore, the design is highly optimised for rated power, without the need to significantly over-engineer the system to cater for excesses above rated power.

Furthermore, the ability of some control systems to adapt the WEC to varying sea conditions may be dictated by the device mass [10], especially in the case of latching, where the device dynamics can be slowed down to match wave of a longer period than the device resonant frequency, but not speeded up. The literature also contains a number of practical studies where doubt is cast over the viability of reactive control schemes, where power *is provided to* the WEC during part of the oscillation cycle, mainly due to the unreasonably large peak to average power ratios involved [11], [12].

Various previous studies have been completed which, to some degree of priority, deal with wave energy variability. The generic issue of uncertainty in wave energy resource assessment has been studied in [13], while specific regional studies which include variability have been reported in [14] and [15] for the northwest European shelf and the Persian Gulf, respectively.

There are, in fact, three wave energy economic impacts of variability. The first, articulated already above, is the increased capital cost of a device via the need to over-engineer the device to operate and survive in sea states in excess of the predominant design state. The second, also a cost item, is the increased cost of maintenance, due to the presence of stresses at the design limit of the system. The third impact is the potential reduction in power quality and possible sanctions imposed by the transmission system operator (particularly in real-time energy markets). The capital and maintenance cost issues are not unconnected. The more robust the device, the greater the capital cost, which leads to lower maintenance. The device/project developer must decide where the tipping point is between the design power point and the maximum extreme likely.

Under most incentivising renewable feed-in tarriffs (REFITs), wave power producers would be paid for each MWh produced, regardless of variability (so long as grid rules are not compromised). However, depending on jurisdiction, real-time energy markets may be more economically advantageous than REFITs. In addition, renewable producers may be slowly weaned off REFITs and forced onto real-time markets. In a real-time market, power producers must make bids for power production over a certain interval (e.g. 30 mins). Failure to supply the bid level results in significant market penalties, while over production results in wasted energy. Thus, reduction in variability of power production is key. Seasonal matching of electrical supply to load may also bring some economic benefits for wave power, depending on the architecture of the electricity market. Seasonal matching is discussed briefly, by way of example, in Section V.

Variability of output power can be reduced by the addition of an energy storage mechanism. Ideally, storage should be located as close to the primary energy source, to minimise the rating requirements of downstream components. Various short- and longer-term storage possibilities for wave energy exist, including hydraulic accumulators for hydraulic power take-off (PTO) systems [16]. On the electrical side, power can be stored/smoothed using supercapacitors [17] , batteries (including flow batteries) or fuel-cell systems [18], and high-inertia flywheels [19]. However, energy storage systems, depending on the point of installation in the power conversion chain, can compromise other control and efficiency maximising measures and carry a significant additional capital and operational cost, in addition to a reduction in overall energy production efficiency. Some non-electrical wave energy applications, such as reverse osmosis, have a natural storage mechanism (i.e. the tank of desalinated water), but also have issues related to the variability of the primary power source [20].

The present paper considers a prototype wave map that is constructed with wave power variability as a central theme. The remainder of the paper is organised as follows: Section II provides a brief enumeration of wave power measures, including variability, while Section III describes the data sources used to construct the new wave map. Section IV introduces the interactive interface to the new wave map, while sample results from the map are shown in Section V. Finally, conclusions are drawn in Section VI.

II. Measures of power

A. *Mean power and energy*

For regular (monochromatic) seas, in deep water, the power (energy flux) transmitted by regular waves, per unit crest width, is given by:

$$P = \frac{1}{32\pi}\rho g^2 H^2 T \tag{1}$$

where ρ is the density of sea water ($\rho \approx 1.028 kg/m^3$), g the acceleration due to gravity ($g = 9.81 m/s^2$), H the wave height (m) and T the wave period (s). Real (panchromatic) seas contain a mixture of a large number of regular waves with varying amplitudes, frequencies and directions. For real seas, an approximate expression for power (energy flux) transmitted, per unit crest width, is:

$$P \approx \frac{1}{64\pi}\rho g^2 H_s^2 T_e \quad (2)$$

where H_s (or $H_{\frac{1}{3}}$) is the significant wave height (the mean of the 1/3 highest waves) and T_e the period of peak energy. The wave power can also be specified in terms of the peak wave period T_p, using the approximate equivalence of:

$$T_e \approx 0.9 T_p \quad (3)$$

assuming a JONSWAP spectrum.

Significantly, we note that wave power increases linearly with period (T or T_p) and quadratically with significant wave height (H or H_s). We note also that wave period and height are statistically linked for a particular location, with an increase in one quantity usually accompanied by an increase in the other. Therefore, moderate increases over the design sea state (H_s, T_p) can result in exponential increases in wave power and contribute to significant power variability.

B. Measures of variability

Many measures of variability are possible, including standard deviation, variance, peak excursion, etc. While standard deviation is a standard statistical measure for assessing the variance of time series, it can difficult to compare for free surface elevation time series with different mean values. As a result, the coefficient of variation (COV) is employed, which is effectively the standard deviation σ normalised by the mean value of the time series, $\overline{P}$, where P is the power measure calculated from (1) or (2). Specifically,

$$COV = \frac{\sigma[P(t)]}{\overline{P(t)}} = \frac{\sqrt{\overline{(P-\overline{P})^2}}}{\overline{P}} \quad (4)$$

It may be noted that, since the COV is normalised by the mean power, the COV is essentially independent of the mean power corresponding to a particular site. However, it should be borne in mind that, for two sites with equal COV, the absolute variance will be larger for the site with the larger mean power.

Seasonal variability, SV, can also be calculated via (5).

$$SV = \frac{P_{max} - P_{min}}{\overline{P}} \quad (5)$$

III. Data collection

A variety of time series data types can be employed to assess power variability, including wave rider buoys and hindcast data from numerical models (usually calibrated with buoy measurements). One requirement is that the data records be sufficiently long to assess short-term, inter-seasonal and inter-annual variability, where possible. Table I summarises the data utilised in the current study, which was kindly supplied for free from a number of data providers and government agencies.

Region	Data source	Company/organization
Europe	ANEMOC [24]	EDF-Cerema
United States	WIS [25]	US Army Corps of Engineers
Chile	Explorador Marino	Chilean Ministry of Energy
Mediterrean Sea	ANEMOC MEDIT [26]	EDF-Cerema
Portugal	Ondatlas [27]	AREAM-LNEG
Iceland	Waveclimate	BTM Argoss
Pacific Islands	WIS [25]	US Army Corps of Engineers
East China Sea	Fugro wave atlas [1]	Fugro OCEANOR

TABLE I
SUMMARY OF DATA SOURCES USED IN THE STUDY

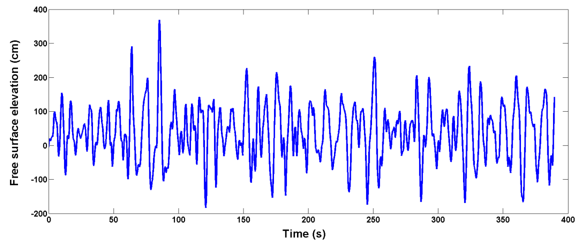

Fig. 2. Free surface elevation variations recorded from a databuoy off the West Coast of Ireland (Data courtesy of the Irish Marine Institute)

A. Buoy data

Data from wave-rider buoys can give a detailed picture of the second-to-second variations in free surface elevation (for example data is recorded at a sampling rate of 2.5 Hz by the Irish Marine Institute Data buoys), while other statistical quantities, such as significant wave height H_s and peak power period T_p, are also calculated on the buoys. However, given the remote location of many of these data buoys (with a resulting restriction of access for maintenance) and the extreme conditions under which they may operate, data drop-outs and sections of missing data are not uncommon. While drop-outs can be addressed using interpolation techniques, sections of missing data may prevent the assessment of inter-season or inter-annual variability, in some cases. Fig.2 shows a typical record for a databuoy off the West Coast of Ireland.

B. Hindcast data

Hindcast data is produced by a wide-scale model for a period in the past. The model output is calibrated with data buoy measurements at specific points, allowing realistic inference to be made over a much wider range than the buoy measurement points. The other advantage of hindcast data is that the model output does not suffer from missing data points, though the calibration data must have good integrity. Typical models used to provide hindcasts include Wavewatch III [28] and TOMAWAC [29]. By way of example, Fig.3 shows a typical hindcast for Arica off the Chilean coast.

IV. User interface

The user interface to the map and data is facilitated by the Google map engine [30]. Each site where data is available is indicated with a marker, with the colour of the marker denoting the COV at that site. Darker markers denote a higher wave energy COV (with the exception of the markers

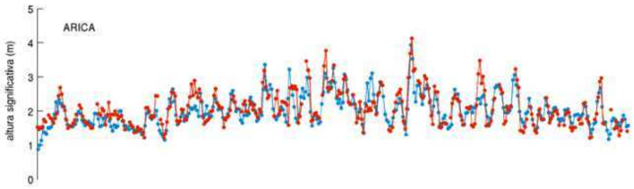

Fig. 3. Hindcast for Arica off the Chilean coast and associated calibration point data (Data courtesy of the Chilean Ministry of Energy)

around Australia, which are placeholders for missing data). The map prototype is shown in Fig.4 and can be accessed at: https://www.google.com/maps/d/viewer?mid=zq3DaeJiEmOQ.kn2zmmo7cahI.

Clicking on one of the markers gives summary information about the point, including:

- Latitude and longitude,
- The nature of the data source, and
- The mean power and COV for the site.

In addition a link is given to a short report for each indicated site, which provides the following information:

- The calculation formula for COV and mean power,
- Plots of the annual COV and mean power for the site,
- A scatter plot of the mean power variations on a monthly basis, and
- A plot of the mean seasonal power variations.

Some examples of these will be shown in Section V.

V. Sample Results

In this section, a variety of results are presented to illustrate the utility of the wave map. In Section V-A, summary results are presented for a wide range of locations, showing the variation in mean power and COV on a global scale. In Section, V-B, typical results from the wave map are presented for a specific location, the Bay of Biscay, in order to demonstrate the range of results possible from the wave map. Finally, in Section V-C, a comparative study is performed which compares two wave energy locations, which have been suggested for development, in terms of variability and mean wave resource.

A. Summary results

Table II gives an overview of the mean wave power and the COV for most of the locations available on the wave map. Where a large number of measurements are available in a relatively small area (e.g. Chile) a sample of results are taken in order to give as clear a global perspective as possible. It is clear that there is a wide variation in mean power between locations, but that the COV does not always scale relative to the mean power. A more useful perspective, perhaps, is obtained from the plot in Fig.5, which shows the mean power plotted against the COV for sites ordered in terms of mean power.

Clearly, Chile, for various sites corresponding to different mean power, is attractive from COV point of view. Indeed,

Location	Source	Period	Mean power	COV
Samoa	WIS	1981-2011	21.2	0.7
Hawaii	WIS	1981-2011	10.3	0.9
Alaska	WIS	1981-2011	67.0	1.3
California	WIS	1981-2011	37.8	1.2
Texas	WIS	1980-2012	4.92	1.6
Alabama	WIS	1980-2012	0.73	2.5
Florida (W)	WIS	1980-2012	1.4	2.8
Florida (E)	WIS	1980-2012	8.91	1.5
N. Carolina	WIS	1980-2012	12.5	1.7
Rhode Is.	WIS	1980-2012	14.8	1.6
Chile (N)	E. Marino	1979-2010	32.3	0.6
Chile (C)	E. Marino	1979-2010	81.3	0.8
Chile (S)	E. Marino	1979-2010	120.9	0.9
Iceland	Waveclimate	1992-2013	64.1	1.5
Scotland	ANEMOC	1979-2002	32.6	1.9
Ireland	ANEMOC	1979-2002	95.3	1.8
Brittany (N)	ANEMOC	1979-2002	12.3	1.8
Brittany (S)	ANEMOC	1979-2002	21.3	2.1
Biscay	ANEMOC	1979-2002	30.5	1.9
France (Med)	ANEMOC	1979-2002	2.91	1.9
Spain (W)	ANEMOC	1979-2002	64.3	1.7
East China S.	FUGRO	1997-2003	12.7	1.8
Guam	WIS	1981-2011	16.3	1.5

TABLE II
SUMMARY DATA FOR ALL LOCATIONS

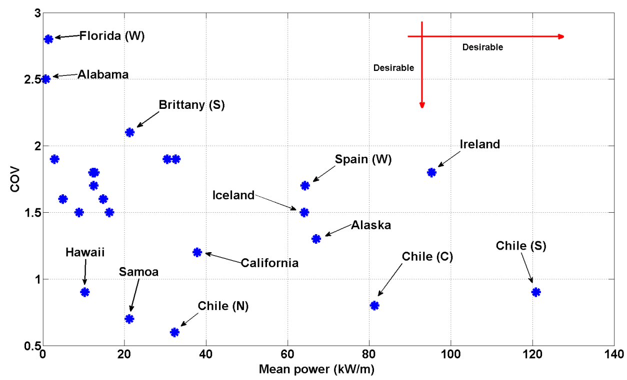

Fig. 5. Mean power and COV for various sites ordered by mean power

a relatively consistent COV is achieved for the three sites plotted for Chile, in spite of a significant range in mean power variation between sites. On the other hand, sites with data points towards the top end of the plot have relatively poor COV figures.

B. Specific location: Bay of Biscay

As mentioned in Section IV, various data are available through the map interface, including plots of the annual COV and mean power for a site, a scatter plot of the mean power variations on a monthly basis, and plot of the mean seasonal power variations. These will now be illustrated for a particular site. The site location, on the French Atlantic Coast, is shown in Fig.6. For this location, data was supplied by the ANEMOC wave atlas [24] with data available from 1979 to 2002. Over this period, the location in question presents an annual mean power of 22 kW/m and a COV of 2.1. As a reference, the COV generally varies between 0.5 and 3, with a value of

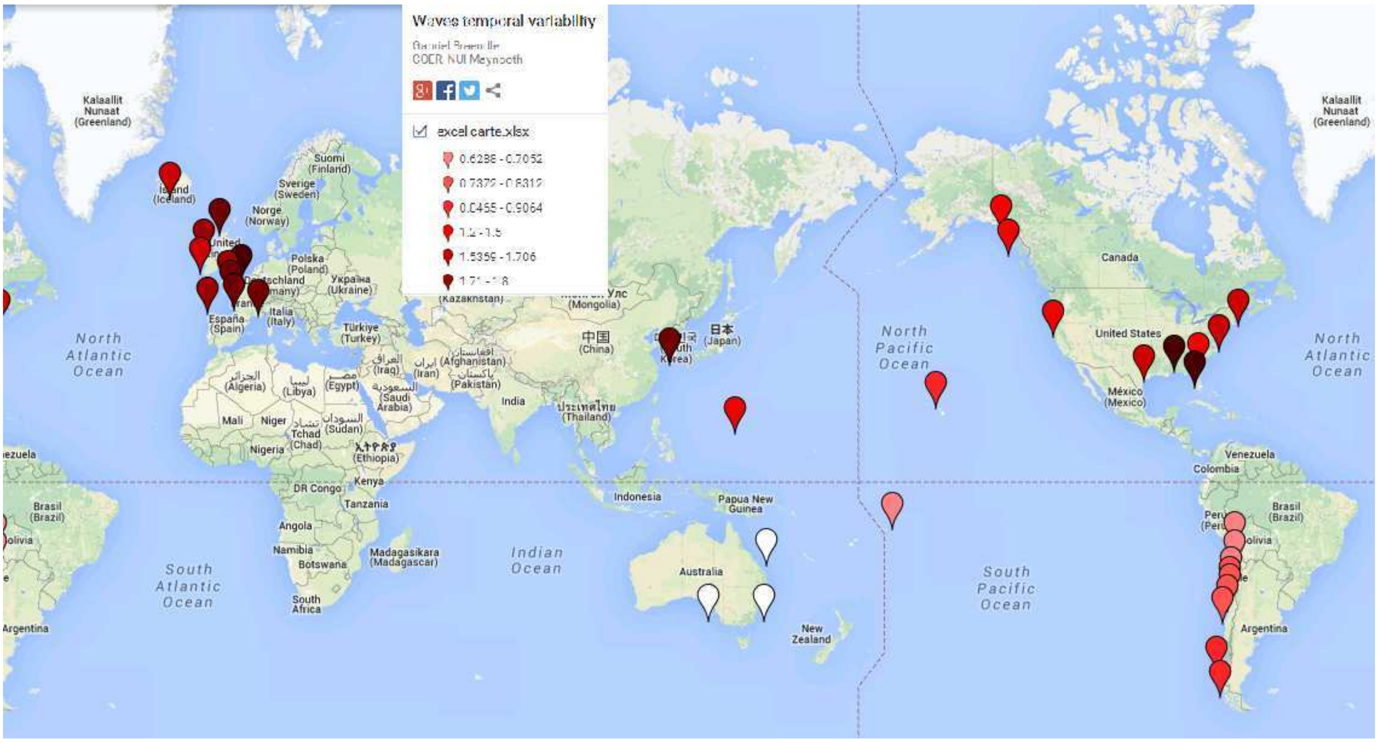

Fig. 4. Interface to interactive world wave energy map which focusses on variability

Fig. 6. Location used for specific site example

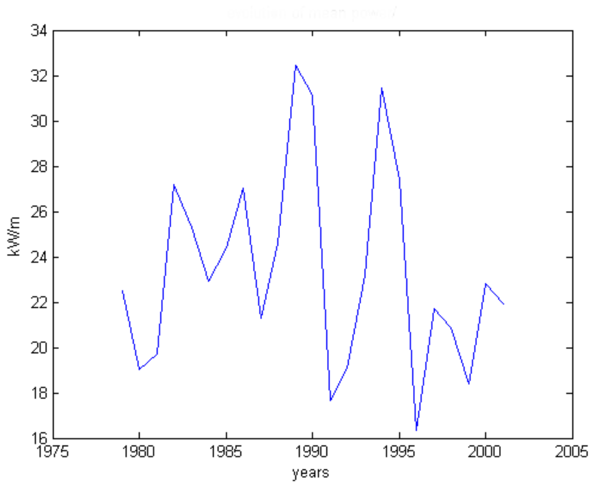

Fig. 7. Annual mean power variations at location 2627

0.5 indicating virtually no variability, while a value of over 2.5 indicated very significant variability. Therefore, a COV of 2.1 indicates moderate variability, but does not give specific information on the timescale on which this variability occurs. However, further data provided by the wave map can give some extra insight.

Fig.7 shows the evolution of the annual mean power at location 2627. There is a considerable difference between the annual max. (32 kW/m) and min. (16 kW/m), consistent with the relatively large COV. The COV itself can also be calculated on an annual basis and the result for location 2627 is shown in Fig.8. Fig.8 shows the the COV itself is not steady, but exhibits significant inter-annual variation. There is also a clear correlation between the annual COV and annual mean power, as shown in Fig.7 (for example see years 1989 and 1994), not least due to the presence of mean power in the COV calculation of (4). The seasonal variability can also be examined, as shown in Fig. 9, which shows the mean power

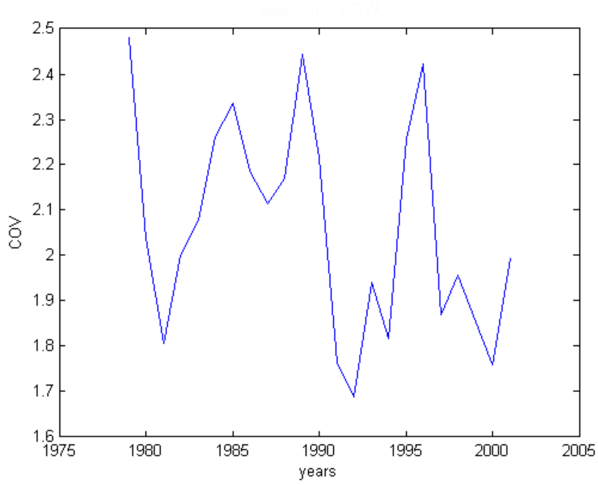

Fig. 8. Annual COV at location 2627

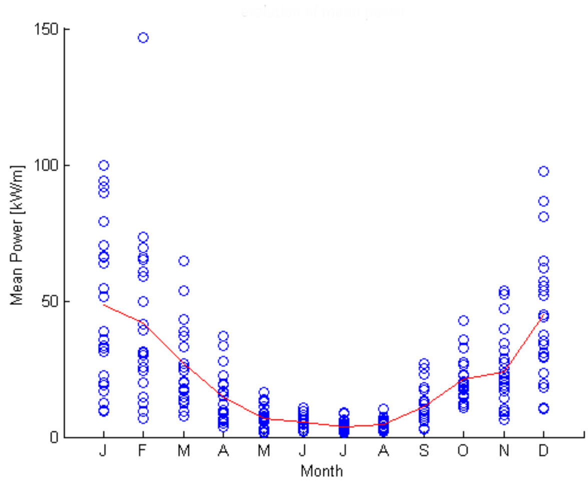

Fig. 10. Scatter plot for monthly variations in mean power at location 2627

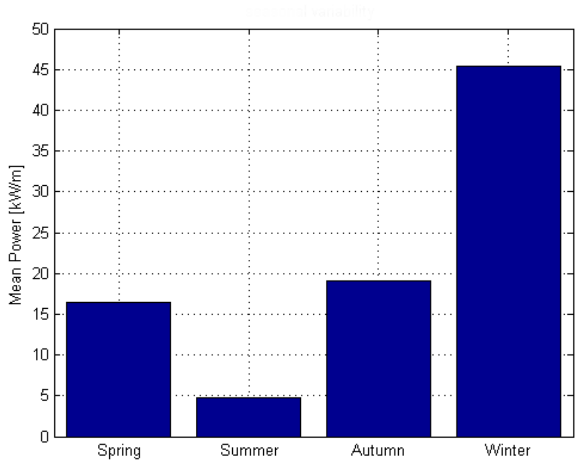

Fig. 9. Season variations in mean power at location 2627

averaged by season. As expected, the max. mean power occurs in winter, at almost a factor of 10 greater than the summer. For some jurisdictions, having a peak in the winter may suit local consumption patterns, where much of the electrical load is due to heating and lighting requirements. However, other locations may experience a significant air conditioning requirement in summer, which would be badly matched to a supply profile as shown in Fig.9. In general, equatorial areas generally have a lower seasonal variability, but also have correspondingly lower mean wave power. Finally, a scatter plot for each highlighted location is also available via the map interface. The scatter plot documents the distribution of the mean power levels on a monthly basis. Since 23 years of data are available for location 2627, 23 datapoints for each month are shown in Fig.10. The solid line shows the mean seasonal variation, consistent with the data shown in Fig.9. As the information is displayed on a finer timescale, extremes in the data begin to manifest themselves. In particular, the individual point for February with a mean power of 150 kW/m is noteworthy.

C. A comparative study: Chile Vs Ireland

Two countries that have realistic aspirations to harness wave power are Chile and Ireland. In this section, the wave resources of the two countries are compared using the wave map. Both countries have a significant resource, but face different oceans, and occupy positions of somewhat similar lattitude (Chile at $18^o \rightarrow 15^o$ South, Ireland at $52^o \rightarrow 55^o$ North), though Chile has a much greater span of latitude than Ireland. Fig.11 shows a section of the wave map for Chile, indicating the points at which wave power measurements are available. Clearly, the marker points darken as movement is made from North to South, indicating that the COV is greater in the Southern latitudes (as is the mean wave power), confirming the reduction is mean and COV towards equatorial regions. Table III summarises the key comparative parameters for both Chile and Ireland, in terms of the available wave resource. Note that seasonal variability (SV) is calculated via (5).

Indicator	Chile	Ireland
Mean power (kW/m)	82	89
COV	0.83	1.7
Highest annual mean power (kW/m)	120	150
Highest monthly mean power (kW/m)	200	500
Seasonal variability	~ 0.45	~ 1.8

TABLE III
COMPARISON OF WAVE POWER INDICATORS FOR CHILE AND IRELAND

A number of comments on Table III are pertinent. Firstly, the mean power values for both countries are very close (82 for Chile Vs 89 for Ireland), indicating a good basis for a comparative evaluation. However, there is significant difference in variability measures. With a COV and VS of 0.83 and 0.45 respectively, Chile has much superior variability indices, which should make Chile more economically attractive for wave power projects, compared to Ireland. This is also borne out by the extreme annual and monthly mean powers of 120

Fig. 11. Wave map section, showing measurement points for Chilean coast, with markers colour coded with COV

kW/m and 200 kW/m, respectively, for Chile compared to the 150 kW/m and 500 kW/m for Ireland.

VI. Conclusions

A new wave map, based on currently available data, has been assembled, focussing on wave power variability. It is a prototype map and is therefore incomplete, but hopefully provides sufficient information to heighten awareness of variability as an important cost driver for converted wave energy. The interface to the map data is interactive and visual and the map data access is hierarchical, with broad summary information (COV as colour-coded icons) provided at the top level. At one level down from the top, summary information including enumeration of COV and mean power, together with an identifier for the data source and latitude and longitude coordinates for the site, are provided. At the lowest level, a mini report, which shows plots of annual, seasonal and monthly variability, is provided.

There is a significant dividend to be gained with the provision of a viable and economic wave power source. However, some indicators in isolation, such as mean wave power (for locations) and efficiency (for devices) can be misleading as key variables upon which to pick ideal wave power locations and technologies. Wave power in its raw state is free, so the chief objective is to minimise the cost of converted wave power. To that end, the authors believe that wave power variability is a key variable to consider. For sites with similar COV, it may be tempting to choose one with a significantly higher mean power; however, this is not always beneficial, since sites with higher mean power normally have reduced weather windows for maintenance/deployment/retrieval, or place more stringent requirements on support vessels or the type of marine operations that can be performed on site.

Nevertheless, there are a number of other factors which will influence the decision with regard to optimal siting of wave energy farms, including the availability of nearby port and other facilities, local bathymetry, frequency of incidence of storms and hurricances (which may have little impact on the COV) and the feed-in tariff offered in various jurisdictions. Ultimately, a large number of factors need to be considered in the total economic benefit analysis of wave farms in various locations.

Acknowledgment

The authors are grateful for the hindcast data utilized in this research project, which were provided free by several organizations:

- ANEMOC [24], [26]: A French atlas developed by a collaboration between EDF RD-LNHE and the Cerema-DTecEMF,
- Wave Information Study [25]: A wave atlas of the United states, built by the US Army Corps of Engineers,
- Ondatlas [27]: Wave atlas for the island of Madeira, built by a collaboration between the Agencia Regional da Energia e Ambiante de Regiao da Madeira (AREAM) and the Laboratrio Nacional de Energia e Geologia (LNEG),
- Explorador Marino: A wave atlas for the Chilean cost built by the Chilean Ministry for Energy,
- Wave Climate: a global wave hindcast built by the compagny BTM ARGOSS with some demonstration points available for free.
- Fugro Oceanor [1]: a global wave hindcast built by the compagny FUGRO OCEANOR with some demonstration points available for free.

In addition, the data provided by the Irish Marine Institute is gratefully acknowledged.

References

[1] G. Mork, S. Barstow, A. Kabuth, and M. Pontes, "Assessing the global wave energy potential," in *Proc. OMAE*, Shanghai, 2010, pp. 447–454.
[2] B. Kinsman, *Wind waves: Their generation and propagation and propagation on the ocean surface*. Courier Corporation, 1965.
[3] D. Mollison, "Wave climate and the wave power resource," in *Hydrodynamics of Ocean Wave-Energy Utilization*. Springer, 1986, pp. 133–156.
[4] K. Gunn and C. Stock-Williams, "Quantifying the global wave power resource," *Renewable Energy*, vol. 44, no. 0, pp. 296 – 304, 2012.

[5] R. A. Arinaga and K. F. Cheung, “Atlas of global wave energy from 10 years of reanalysis and hindcast data,” *Renewable Energy*, vol. 39, no. 1, pp. 49 – 64, 2012.

[6] H. L. Tolman, “The 2002 release of wavewatch iii,” in *7th International Workshop on Wave Hindcasting and Forecasting*, 2002, pp. 188–197.

[7] J. Hanson and O. Phillips, “Automated analysis of ocean surface directional wave spectra,” *Journal of Atmospheric and Oceanic Technology*, vol. 18, no. 2, pp. 277–293, 2001.

[8] S. Ocean, “Ocean energy: Cost of energy and cost reduction possibilities,” Intelligent Energy Europe, Tech. Rep., 2013.

[9] B. Teillant, R. Costello, J. Weber, and J. Ringwood, “Productivity and economic assessment of wave energy projects through operational simulations,” *Renewable Energy*, vol. 48, pp. 220–230, 2012.

[10] S. Astariz and G. Iglesias, “The economics of wave energy: A review,” *Renewable and Sustainable Energy Reviews*, vol. 45, pp. 397–408, 2015.

[11] J. Sjolte, G. Tjensvoll, and M. Molinas, “Power collection from wave energy farms,” *Applied Sciences*, vol. 3, no. 2, pp. 420–436, 2013.

[12] W. Kellogg, M. Nehrir, G. Venkataramanan, and V. Gerez, “Generation unit sizing and cost analysis for stand-alone wind, photovoltaic, and hybrid wind/pv systems,” *IEEE Transactions on Energy Conversion*, vol. 13, no. 1, pp. 70–75, 1998.

[13] A. Clément, P. McCullen, A. Falcão, A. Fiorentino, F. Gardner, K. Hammarlund, G. Lemonis, T. Lewis, K. Nielsen, S. Petroncini *et al.*, “Wave energy in europe: current status and perspectives,” *Renewable and sustainable energy reviews*, vol. 6, no. 5, pp. 405–431, 2002.

[14] J. Ringwood, G. Bacelli, and F. Fusco, “Energy maximising control of wave energy converters,” *IEEE Control Systems Magazine*, vol. 34, no. 5, pp. 30–55, 2014.

[15] J. K.-H. Shek, D. E. Macpherson, M. A. Mueller, and J. Xiang, “Reaction force control of a linear electrical generator for direct drive wave energy conversion,” *IET renewable power generation*, vol. 1, no. 1, pp. 17–24, 2007.

[16] J. Sjolte, C. M. Sandvik, E. Tedeschi, and M. Molinas, “Exploring the potential for increased production from the wave energy converter lifesaver by reactive control,” *Energies*, vol. 6, no. 8, pp. 3706–3733, 2013.

[17] E. B. Mackay, A. S. Bahaj, and P. G. Challenor, “Uncertainty in wave energy resource assessment. part 2: variability and predictability,” *Renewable Energy*, vol. 35, no. 8, pp. 1809–1819, 2010.

[18] S. P. Neill and M. R. Hashemi, “Wave power variability over the northwest european shelf seas,” *Applied Energy*, vol. 106, pp. 31–46, 2013.

[19] B. Kamranzad, A. Etemad-Shahidi, and V. Chegini, “Assessment of wave energy variation in the persian gulf,” *Ocean Engineering*, vol. 70, pp. 72–80, 2013.

[20] G. Nolan, M. O Cathain, J. Murtagh, and J. Ringwood, “Modelling and simulation of the power take-off system for a hinge-barge wave-energy converter,” in *Proc. Fifth European Wave Energy Conference, Cork, Ireland*, 2003.

[21] Z. Zhou, M. Benbouzid, J. F. Charpentier, F. Scuiller, and T. Tang, “A review of energy storage technologies for marine current energy systems,” *Renewable and Sustainable Energy Reviews*, vol. 18, pp. 390–400, 2013.

[22] P. J. Hall and E. J. Bain, “Energy-storage technologies and electricity generation,” *Energy policy*, vol. 36, no. 12, pp. 4352–4355, 2008.

[23] B. Bolund, H. Bernhoff, and M. Leijon, “Flywheel energy and power storage systems,” *Renewable and Sustainable Energy Reviews*, vol. 11, no. 2, pp. 235–258, 2007.

[24] G. Bacelli, J.-C. Gilloteaux, and J. Ringwood, “A predictive controller for a heaving buoy producing potable water,” in *Proceedings of the 10^{th} European Control Conference, Budapest, Hungary*, 2009, pp. 3755–3760.

[25] G. Mattarolo, F. Lafon, and M. Benoit, “Wave energy resource off the french coasts: the anemoc database applied to the energy yield evaluation of wave energy converters,” in *Proceedings of the 8th European wave and tidal energy conference*, 2009, pp. 247–55.

[26] J. M. Hubertz, *User's guide to the Wave Information Studies (WIS) wave model, version 2.0*. US Army Engineer Waterways Experiment Station, 1992, vol. 27.

[27] D. Morellato and M. Benoit, “Constitution of a numerical wave database along the french mediterranean coasts through hindcast simulations over 1979–2008,” in *MMX CONGRESS*, 2010.

[28] M. T. Pontes, R. Aguiar, and H. O. Pires, “A nearshore wave energy atlas for portugal,” *Journal of Offshore Mechanics and Arctic Engineering*, vol. 127, no. 3, pp. 249–255, 2005.

[29] M. Benoit, F. Marcos, and F. Becq, “Tomawac: a prediction model for offshore and nearshore storm waves,” in *Proc. Int. Assoc. for Hydraulic Research Congress*, 1997, pp. 1316–1321.

[30] C. C. Miller, “A beast in the field: The google maps mashup as gis/2,” *Cartographica: The International Journal for Geographic Information and Geovisualization*, vol. 41, no. 3, pp. 187–199, 2006.